Farnesylthiosalicylic Acid-derivatized PEI-based Nanocarrier for Improved Tumor Vaccination

by

Yuang Chen

BS, University of Pittsburgh, 2017

Submitted to the Graduate Faculty of

School of Pharmacy

of the requirements for the degree of

Master of Science

University of Pittsburgh

2020

UNIVERSITY OF PITTSBURGH

SCHOOL OF PHARMACY

This thesis/dissertation was presented

by

Yuang Chen

It was defended on

April 3, 2020

and approved by

Song Li, Professor, Department of Pharmaceutical Science

Binfeng Lu, Associate Professor, Department of Immunology

Xiaochao Ma, Associate Professor, Department of Pharmaceutical Science

Thesis Advisor/Dissertation Director: Song Li, Professor, Department of Pharmaceutical Science

Farnesylthiosalicylic Acid-derivatized PEI-based Nanocarrier for Improved Tumor Vaccination

Yuang Chen, BS

University of Pittsburgh, 2020

Vaccines hold huge potential for cancer immunotherapy by activating and stimulating our immune system. Cancer vaccines that make use of mutant tumor antigens represent a promising therapeutic strategy by stimulating immune responses against tumors to generate long-term anti-tumor immunity. However, vaccines have shown limited clinical efficacy in high risk cancer patients, which mostly due to the inefficient delivery. In this study, we will focus on vaccine delivery assisted by nanoparticles for cancer immunotherapy. Nanoparticle-mediated vaccination can efficiently deliver neoantigenic nucleic acids into lymphoid organs and antigen presenting cells. The intracellular release of vaccine and cross-presentation of antigens can be fine-tuned via polymer engineering. Polyethylenimine (PEI) was conjugated with farnesylthiosalicylic acid (FTS), an inhibitor of RAS signaling and the resulting amphiphilic conjugate could self-assemble to form micelles. Subsequent interaction with nucleic acids led to formation of polymer/nucleic acid complexes of well-controlled structure. Tumor transfection via PEI-FTS was much more effective than that by PEI, other PEI variants or naked DNA alone. Significant transfection was also observed in draining lymph nodes. *In vivo* delivery of an ovalbumin (OVA, a model antigen) expression plasmid by PEI-FTS led to a significant growth inhibition of OVA-expressing B16F10 melanoma. PEI-FTS represents a promising transfection agent for effective gene delivery to tumors and draining lymph nodes to mediate neoantigen vaccination.

Table of Contents

List of Figures

List of Supplementary Figures

1.0 Introduction

Vaccines that activate our immune system for prevention and treatment of infections and other diseases have played a significant role in human healthcare[1]. Cancer neoantigens from somatic mutations in tumor tissues provide an attractive target for cancer immunotherapies such as cancer vaccine[2]. Vaccination against tumor-specific neoantigens has the capability to decrease the induction of potential central and peripheral tolerance and various autoimmune diseases[3, 4]. It has reported that neoantigen-based personalized vaccination shows remarkable therapeutic potential in preclinical and early-phase clinical studies[5-7]. However, significant challenges remain in the efficient and safe delivery of the vaccine components to induce potent and generalized anti-cancer T cell responses[8].

Our long-term goal is to develop a simple and effective vaccination strategy. It will be based on the concept that tumors have mutations and these mutant epitopes can be immunogenic[9-12]. If the mutation can be identified, packed into a plasmid expression system, delivered and expressed in professional antigen presenting cells (APCs) such as macrophages (MΦs) and dendritic cells (DCs), significant immune response could be induced to attack the mutated cancer cells[13].

Currently, a variety of delivery systems have been developed for gene delivery including viral and non-viral carriers[14]. Various non-viral systems have been reported including peptides, liposomes and cationic polymers[15]. Non-viral nanoparticles have attracted increasing attention in nucleic acid delivery due to their favorable safety profiles and the ease of production[14-17]. Nanoparticles have been extensively investigated for vaccine delivery since they could protect vaccines from degradation, prolong retention time and enhance lymphoid organ targeting[18].

We herein developed a delivery system based on polyethylenimine (PEI), a cationic polymer that has been used widely in non-viral gene delivery including intratumor injection[19]. PEI has a high charge density with proton sponge effect. Unprotonated secondary amines of PEI absorb protons as they are internalized into the endosome, resulting in more protons being pumped in and increased influx of Cl^- ions and water[20]. This can lead to endosomal bursting and the subsequent release of endocytosed materials into cytosol[19]. PEI is a water-soluble molecule that can randomly interact with nucleic acids in aqueous solutions. By anchoring PEI molecules on the surface of nanoparticles of defined sizes, a more effective and controllable interaction with nucleic acids can be achieved[21]. We conjugated Farnesylthiosalicylic acid (FTS) with PEI to form amphiphilic molecules that self-assembled to form micellar nanoparticles. PEI served as the cationic hydrophilic domain to bind nucleic acid and increase cellular uptake. Water-insoluble drug FTS served as the hydrophobic region of polymeric micelles. FTS is a nontoxic RAS antagonist and can inhibit receptor-mediated RAS activation, resulting in the inhibition of RAS-dependent tumor growth[14].

We hypothesized that intratumor delivery of a tumor neoantigen expression plasmid assisted by a cationic polymer can mobilize immunity against a broad range of cancer mutations[22, 23]. This study mainly focused on the synthesis and characterization of a new cationic polymer, testing its *in vitro* and *in vivo* transfection efficiency. In addition, ovalbumin (OVA) was used as a model antigen to examine antigen presentation and nanoparticle-mediated vaccination[24]. Neoantigenic vaccination has the capability of not only expanding the population of pre-existing neoantigen specific T cells, but also inducing a wider range of T cells of new characteristics and functions in cancer treatment, pushing the intra-tumoral balance towards enhancing anti-tumor immunity and better tumor control[1, 25].

2.0 Methods

2.1 Materials

Polyethylenimine (PEI) was purchased from Polysciences (PA, U.S.A.). Farnesylthiosalicylic acid (FTS) was synthesized and purified following a published literature[14]. Dulbecco's Modified Eagle's Medium (DMEM) and trypsin-EDTA solution were purchased from Sigma-Aldrich (MO, U.S.A). HiScribe T7 ARCA mRNA Kit (with tailing) was purchased from New England BioLabs (MA, U.S.A). Pierce® Firefly Luciferase Glow Assay Kit and Pierce™ RIPA buffer were purchased from Thermo Scientific (MA, U.S.A). Ovalbumin Polyclonal Antibody, fetal bovine serum (FBS) and penicillin-streptomycin solution were purchased from Invitrogen (NY, U.S.A.).

2.2 Animals and Cells

Female BALB/c mice (4–6 weeks) were purchased from Charles River (CA, U.S.A) and female C57BL/6J mice (4-6 weeks) were purchased from The Jackson Laboratory (ME, U.S.A). All animals were housed under pathogen-free conditions according to AAALAC (Association for Assessment and Accreditation of Laboratory Animal Care) guidelines. All animal-related experiments were performed in full compliance with institutional guidelines and approved by the Animal Use and Care Administrative Advisory Committee at the University of Pittsburgh.

Murine colorectal carcinoma cell line CT26, triple negative breast carcinoma cell line 4T1.2 and melanoma cell line B16F10 were obtained from ATCC (VA, U.S.A). 4T1.2-tdTomato cell line was kindly given by Dr. Da Yang Lab. Ovalbumin (OVA)-expressing B16F10 mouse melanoma cell line is generated by transfection of B16F10 cell line with OVA plasmid and by G418 selection. All cell lines used in this work were cultured in DMEM medium supplemented with 10% FBS and 1% penicillin/ streptomycin at 37 °C in a humidified atmosphere with 5% CO_2. All cell lines were subject to periodic testing for mycoplasma using the LookOut Mycoplasma PCR detection kit (Sigma).

2.3 Synthesis of Polymers

PEI-FTS was synthesized via solution condensation reactions from linear PEI (Mw = 2500 Da or 25000 Da). PEI (129 mg, 3 mmol –NH-) was reacted with FTS at different ratio (10.74 mg, 0.03 mmol; 53.7 mg, 0.15 mmol) in DMF (5mL) at room temperature under stirring, N,N′-Dicyclohexylcarbodiimide (DCC, same equivalent to FTS) was used as condense reagent, and DMAP (5 mg) was used as a catalyst. After 16 h, the reaction mixture was filtered by cotton, followed by adding 50 mL diethyl ether. The mixture was centrifuged at 4500 rpm for 10 min. Then, the PEI-FTS polymer was obtained by precipitation in ether for 3 times.

2.4 Preparation and Characterization of Nucleic Acid-loaded Micelles

Nucleic acids such as plasmid DNA (0.5mg/mL in distilled deionized (DD) water) or mRNA (0.2mg/mL in DD water) was mixed with PEI-FTS micelles (2mg/mL in DD water) at desired N/P ratios. Nanocomplexes were allowed to incubate at RT for 20 min prior to further characterization. Both *in vitro* and *in vivo* studies were performed with freshly prepared nanocomplexes.

The particle size and zeta potential of nucleic acid-loaded PEI-FTS nanocomplexes at different N/P ratios were assessed by dynamic light scattering (DLS) via a Zetasizer (Nano ZS instrument, Malvern, Worcestershire, U. K.). For gel retardation assay, nucleic acid-loaded nanocomplexes were prepared at different N/P ratios and then electrophoresed on a 2% agarose gel. The gels were prepared with 2% agarose in Trisacetate-EDTA (TAE) buffer containing 0.5 μg/mL ethidium bromide (Biotium, CA, U.S.A). BlueJuice™ Gel Loading Buffer (10X) (Invitrogen, NY, U.S.A). Gel electrophoresis was carried out at 120 V for 20 min and the gel was subsequently visualized using a UV illuminator. Free nucleic acid was served as a control.

2.5 Transfection of Nanocomplexes

Transfection of fluorescence-labelled nucleic acid-loaded PEI-FTS nanocomplexes was evaluated by using confocal laser scanning microscopy (CLSM, FluoView 1000, Olympus, Japan). For *in vitro* validation, cells were seeded in 6-well plates at a density of $2 \times 10_4$ cells/ well followed by 24 h of incubation in DMEM containing 10% FBS and 1% streptomycin/ penicillin. The cells were then treated with EGFP-loaded nanocomplex with different N/P ratios in Opti-MEM

medium. Free EGFP plasmid was used as control. The cells were washed three times with cold DPBS to remove the remaining nanocomplexes after 24 h. Cell nuclei were then stained with Hoechst 33342 (1 μg/mL) at RT for 15 min. Cells were then washed with cold DPBS three times before observation under a confocal scanning microscope. For *in vivo* validation, female BALB/c mice aged 4-6 weeks were inoculated subcutaneously with CT26 cells ($5\times10_5$) or 4T1.2-tdTomato cells ($1\times10_5$) into the right flank. Mice were given intratumor injection of PEI-FTS nanocomplexes loaded with 50 μg EGFP plasmid on day 6 after tumor inoculation. Mice were sacrificed 48 h later; tumor tissues were taken out and cut into frozen sections before detection under a confocal scanning microscope.

2.6 Western Blotting

Western blotting was performed to evaluate OVA expression in B16F10-OVA stable cell line. Cultured cells were harvested and lysed with RIPA lysis buffer (Thermo Fisher Scientific, MA, U.S.A) by gently shaking on ice for 30 min. After centrifugation at 12,500 g for 10 min, the supernatants were collected and the concentrations of proteins were measured using Pierce BCA Protein Assay Kit (ThermoFisher Scientific, MA, U.S.A). The protein samples were denatured by boiling for 5 min and loaded onto 10% SDS-PAGE gel for electrophoresis. The proteins were then incubated in blocking buffer (5% non-fat dry milk in TBST) at RT for 1 h after being transferred onto PVDF membranes (Bio-Rad, CA, U.S.A). The membranes were then incubated with anti-OVA polyclonal antibody in antibody dilution buffer (5% BSA in TBST) with gentle agitation overnight at 4 °C. After washing with TBST for three times, the membranes were subsequently incubated with the secondary HRP-linked goat anti-rabbit IgG antibody (Cell Signaling

Technology, MA, U.S.A) at RT for 1 h. After another three washes washing with TBST, the membranes were incubated with Pierce™ ECL Western Blotting Substrate (Thermo Fisher Scientific, MA, U.S.A) for 1 min, wrapped in plastic and exposed to X-ray film. Protein expression was normalized against GAPDH or β-Actin expression.

2.7 Immunization and Anti-tumor Efficacy

Female C57BL/6J mice aged 4–6 weeks were inoculated subcutaneously with B16F10-OVA cells ($1\times10_5$) into the right flank. Vaccination timelines were selected based on the growth curves of the mouse models and according to literature descriptions. Vaccinations began when tumor sizes were less than 50 mm_3 (or on day 6 after tumor inoculation). Mice were immunized by intratumor injection of PEI-FTS nanocomplexes loaded with 50 μg OVA DNA (dOVA) or 20 μg OVA mRNA (mOVA), as described in the main text. Three doses were given every 6 d. For the re-challenge model, tumor-bearing vaccinated or nonvaccinated mice were re-challenged by subcutaneous inoculation of $1\times10_5$ B16F10-OVA cells per mouse into the contralateral side of the initial injection site, 22 days from the initial inoculation or 1 d after third and final vaccination. Tumor inhibition was compared with mice bearing freshly inoculated tumors (no previous challenges). Tumors were measured every three days beginning on day 2 after challenge until time of death. Death was defined as the point at which a progressively growing tumor reached 2.0 cm in the longest dimension. Measurements were taken manually by collecting the longest dimension (length) and the longest perpendicular dimension (width). Tumor volume was estimated with the formula: $(L \times W_2) / 2$. CO_2 inhalation was used to euthanize mice on the day of euthanasia. Optimal group sizes were determined empirically.

2.8 Immune Cell Infiltration Profile in Tumors

Tumor infiltrating immune cell population after treatments was conducted in an independent *in vivo* study. Mice received similar treatments as described in the therapeutic study. Twenty-four hours after the last vaccination, tumors and spleens were collected in serum free RPMI medium. Tumors were cut mechanically with scissors and digested with Liberase TL and DNase I. Tissues were further grinded and filtered through a 70 mm cell strainer with red blood cells lysed by ACK lysis buffer. Tumor infiltrating lymphocytes (TILs) and myeloid cells were then purified and stained with fluorescence-labeled antibody purchased from BioLegend, eBioscience and BD for flow cytometry analysis.

For the flow cytometry analysis of surface markers, cells were stained on ice with fluorophore-conjugated antibody. For the staining of intracellular markers, for example, IFN-γ, cells were pre-stimulated with the Cell Stimulation Cocktail (eBioscience) for 6 h, fixed and permeabilized using the fixation/permeabilization solution kit (BD). Then, cells were stained with anti-IFN-γ or other antibodies. Flow data were acquired on a BD LSR II flow cytometer or Cytek Aurora cytometer and analyzed using FlowJo software.

2.9 Statistical Analysis

A two-tailed student's t-test or a one-way analysis of variance (ANOVA) was performed when comparing two groups or more than two groups, respectively. Statistical analysis was performed using Microsoft Excel and Prism 7.0 (GraphPad). Data are expressed as means ± SEM

Difference was considered to be significant if $P < 0.05$ (*$P < 0.05$, **$P < 0.01$, ***$P < 0.001$, ****$P < 0.0001$ unless otherwise indicated).

3.0 Results

3.1 Synthesis and Characterization of PEI-FTS Micelles

The synthesis route of PEI-FTS polymer is shown below (Fig. 1). Farnesylthiosalicylic acid (FTS) was conjugated to polyethylenimine (PEI) via solution condensation reactions.

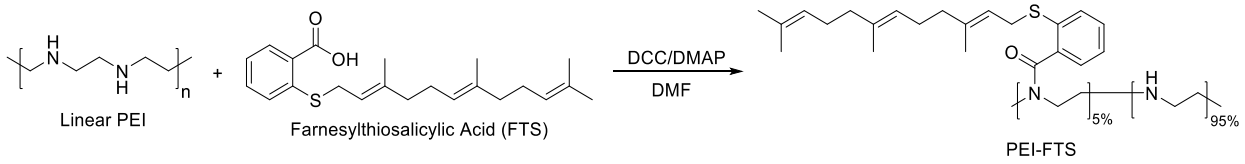

Figure. 1 Synthesis Scheme of PEI-FTS Polymers

PEI-FTS was synthesized via solution condensation reactions from linear PEI. PEI was reacted with FTS at different ratios in DMF at room temperature under stirring, DCC was used as condense reagent, and DMAP was used as a catalyst.

The hydrodynamic sizes of blank PEI-FTS micelles and nucleic acid-loaded PEI-FTS micelles at 0.5/1, 1/1 and 2.5/1 N/P ratios were examined by dynamic light scattering (Fig. 2). PEI-FTS conjugate formed micelles with a size around 160 nm and slightly positive surface charge. After complexing with nucleic acid, micelle size decreased to around 130 nm. The surface charge gradually increased with the increase of N/P ratio. Relatively low N/P ratios were chosen for local delivery since previous literatures reported that a loose complex has better *in vivo* transfection efficiency if administered via intratumor injection.

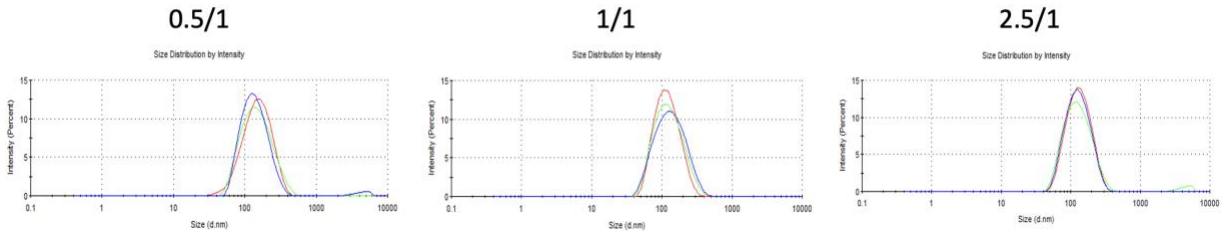

Figure. 2 DLS Characterization of PEI-FTS Micelles

The hydrodynamic sizes of nucleic acid-loaded PEI-FTS micelles were examined by dynamic light scattering (DLS). After complexing with nucleic acid, micelle size is around 130.2 nm at 0.5/1 N/P ratio, 126.3 nm at 1/1 N/P ratio and 139.1 nm at 2.5/1 N/P ratio. The surface charge increased gradually with the increase of N/P ratio.

3.2 PEI-FTS Nanocomplexes-Mediated Nucleic Acid Delivery

Using EGFP as the reporter gene, we first evaluated the nucleic acid delivery efficacy of several polymer conjugates by loading EGFP plasmid into nanocomplexes and comparing GFP protein expression in tumor tissues. Linear PEI (Mw = 2.5k Da or 25k Da) conjugated with different percentage of FTS [W = 10.74 mg, 0.03 mmol (1%) or 53.7 mg, 0.15 mmol (5%)] were complexed with EGFP plasmid at an N/P ratio of 0.5/1, 1/1 and 2.5/1. A total of 12 nanocomplexes were obtained that vary in the FTS/PEI (m/m) as well as N/P ratios. They were individually administered via intratumor injection into tumor bearing mice and tumor tissues were collected after 48 h. Widespread transgene expression was observed in tumor tissues from nanocomplex with a PEI of 2.5k Da and 5% FTS conjugation at a 1/1 N/P ratio. Tumor transfection from PEI-FTS nanocomplex was much more effective than that by PEI or naked DNA alone. (Fig. 3).

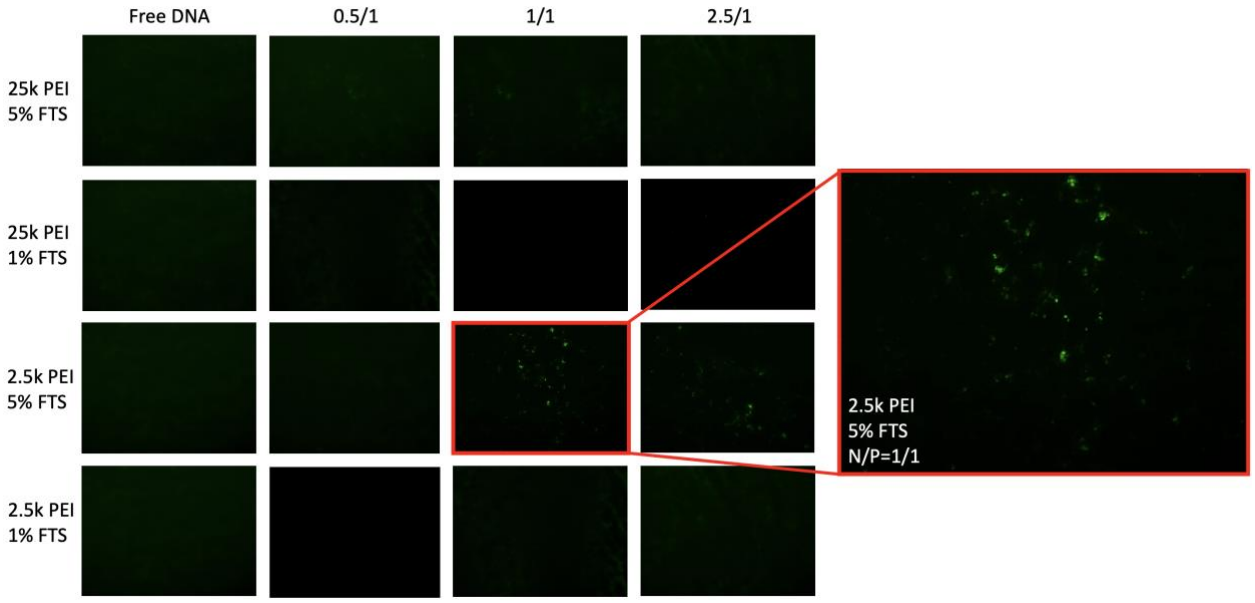

Figure. 3 Screening of PEI-FTS Nanocomplexes

Linear PEI (Mw = 2.5k Da or 25k Da) conjugated with different percentage of FTS [W = 10.74 mg, 0.03 mmol (1%) or 53.7 mg, 0.15 mmol (5%)] were complexed with EGFP plasmid at an N/P ratio of 0.5/1, 1/1 and 2.5/1. A total of 12 nanocomplexes (alongside with free DNA control) were obtained vary in the FTS/PEI (m/m) as well as N/P ratios. Nanocomplexes were individually administered via intratumor injection into tumor bearing mice, tumor tissues were collected after 48 h and transfection efficiency were evaluated by EGFP fluorescence intensity.

We further confirmed the expression of EGFP via immunofluorescence using an EGFP-specific antibody. We observed highly overlapping signals between the green fluorescence signal and EGFP-specific staining signal (red), ruling out the possibility of autofluorescence from the tissues (Fig. 4A). We further confirmed and quantified the gene expression using luciferase as a reporter. Again, the highest level of gene expression was achieved with the nanocomplex with a PEI of 2.5k Da and 5% FTS conjugation at a 1/1 N/P ratio (Fig. 4B). Also, compare to PEI alone,

or PEI modified with other lipid motifs, like OA and lithocholic acid (LA), PEI modified with FTS was much more effective in transfecting tumor (Fig. 4C).

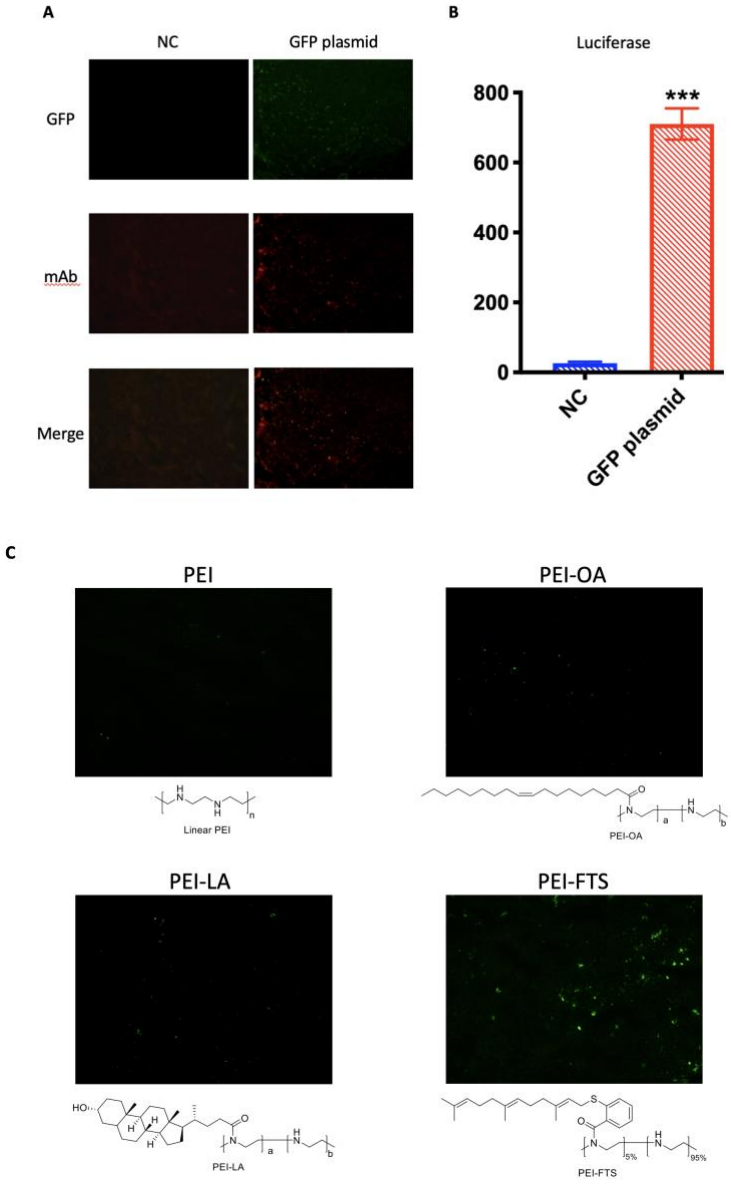

Figure. 4 Transfection Efficiency of PEI-FTS Nanocomplexes and PEI Variants

(A) Immunofluorscence staining of EGFP after 48 h in tumor tissues. (B) Luciferase expression after 48 h in tumor tissues. Statistical analysis and data are presented as the means ± SEM, n = 3. P values were generated by two-tailed student's t-test. *P < 0.05, **P < 0.01, ***P < 0.001. (C) Comparison of chemical structures and EGFP transfection efficiency in tumor tissues between PEI-FTS, PEI alone, PEI-OA and PEI-LA after 48 h.

3.3 PEI-FTS Nanocomplexes Exhibit Specific Tissue and Cell Targeting

Effective nucleic acid-based vaccination requires efficient intracellular antigen expression and pursuant immune cell activation to generate effective immune response. Therefore, we went to examine the other target tissues of the *in vivo* delivery of our nanocomplex besides tumor. Significant transfection was also observed in adjacent draining inguinal lymph node (IN LN) (Fig. 5A). This finding suggests the vaccination potential of our lead nanocomplex since dendritic cells (DCs), which are believed to be one of the main target cells of vaccination due to their capability of antigen presentation and T cell activation, reside mostly in draining LNs.

To determine whether antigen presenting cells (APCs), especially DCs were transfected within tumor and lymph nodes, we delivered both EGFP DNA- or mRNA-loaded PEI-FTS nanocomplex to the 4T1.2-tdTomato-bearing mice. The fluorescence-labelled 4T1.2 tumor cells harbor a stable transfection and express tdTomato. Our results indicated that mRNA induced greater levels of EGFP expression compared to DNA and were able to transfect both tumor cells (tdTomato$_+$) and DCs (CD11b$_+$, MHC II$_+$) (Fig. 5B).

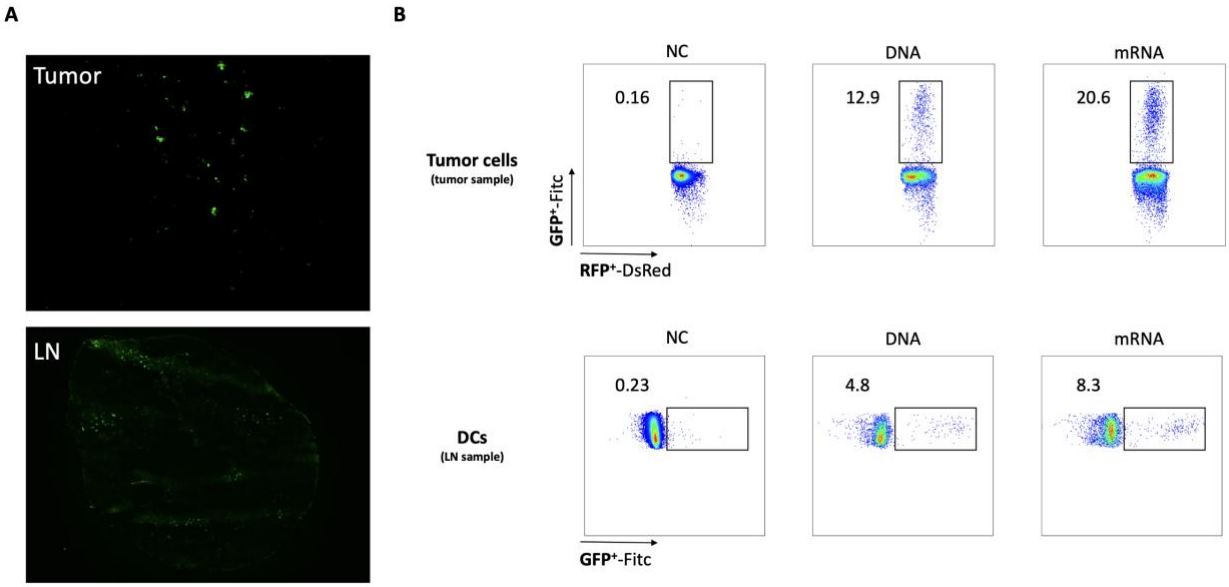

Figure. 5 PEI-FTS Nanocomplexes Exhibit Specific Tissue and Cell Targeting

(A) EGFP expression after 48 h in tumor tissues and draining lymph nodes. (B) FACS analyses of GFP expression in fluorescence-labelled tumor cells (tdTomato^{+}) in tumor tissues and DCs (CD11b^{+}, MHC II^{+}) in draining lymph nodes. *Gating strategy (Fig. S1):* Tumor cells were first gated under Zombie NIR^{-} & CD45^{-} cell population and further characterzied by tdTomato^{+} expression. DCs were first gated under Zombie NIR^{-} & CD45^{+} cells as myeloid cell population and then further characterized by using Gr-1^{-}, CD11b^{+} & MHCII^{+} gating.

3.4 PEI-FTS Nanocomplexes-Mediated Anti-tumor Immunity

The above studies clearly showed the efficacy of our nanocarrier in gene delivery to both tumor cells and antigen presenting cells. As an initial step to test whether delivery of an antigen expression system via our nanocarrier will lead to effective vaccination, Ovalbumin (OVA) was used as a model antigen. We tested the adaptive immune response and anti-tumor efficacy of our nanocomplex delivery systems by establishing an OVA-expressing B16F10 mouse melanoma cell line and delivering an OVA DNA (dOVA) or OVA mRNA (mOVA) vaccine through intratumor administration. We found that OVA-loaded nanocomplex vaccine induced robust tumor suppression with only three doses (once per 6 d) throughout the whole treatment, and tumor sizes were contained at around 200 mm^3 for more than 40 d. Free OVA showed a modest antitumor activity, while empty vector-loaded nanocomplex and PBS control showed almost no anti-tumor efficacy in the B16F10-OVA mouse melanoma model (Fig. 6A). When the OVA loaded nanocomplex was co-delivered with MSOP, a metabotropic glutamate receptor 4 (G4) antagonist, the overall antitumor activity was slightly improved (Fig. 6B).

Finally, by using a tumor re-challenge model, we examined the systemic durability of T-cell responses following vaccination with OVA-loaded nanocomplex. Tumors were inoculated on the contralateral side of the primary tumor following its last immunization. Unfortunately, despite the successful containment of the primary tumor, the growth of the distant tumor was poorly controlled, suggesting that our vaccination approach was only effective in inducing local antitumor immunity (Fig. 6C). Flow cytometry analysis were performed to identify tissue-resident T cells that do not recirculate and expresses specific markers of residency ($CD103^+$ and $CD69^+$) (Fig. 6D). There was a significant increase of tumor infiltrating tissue-resident T cell percentage in primary tumors compared to re-challenge tumors.

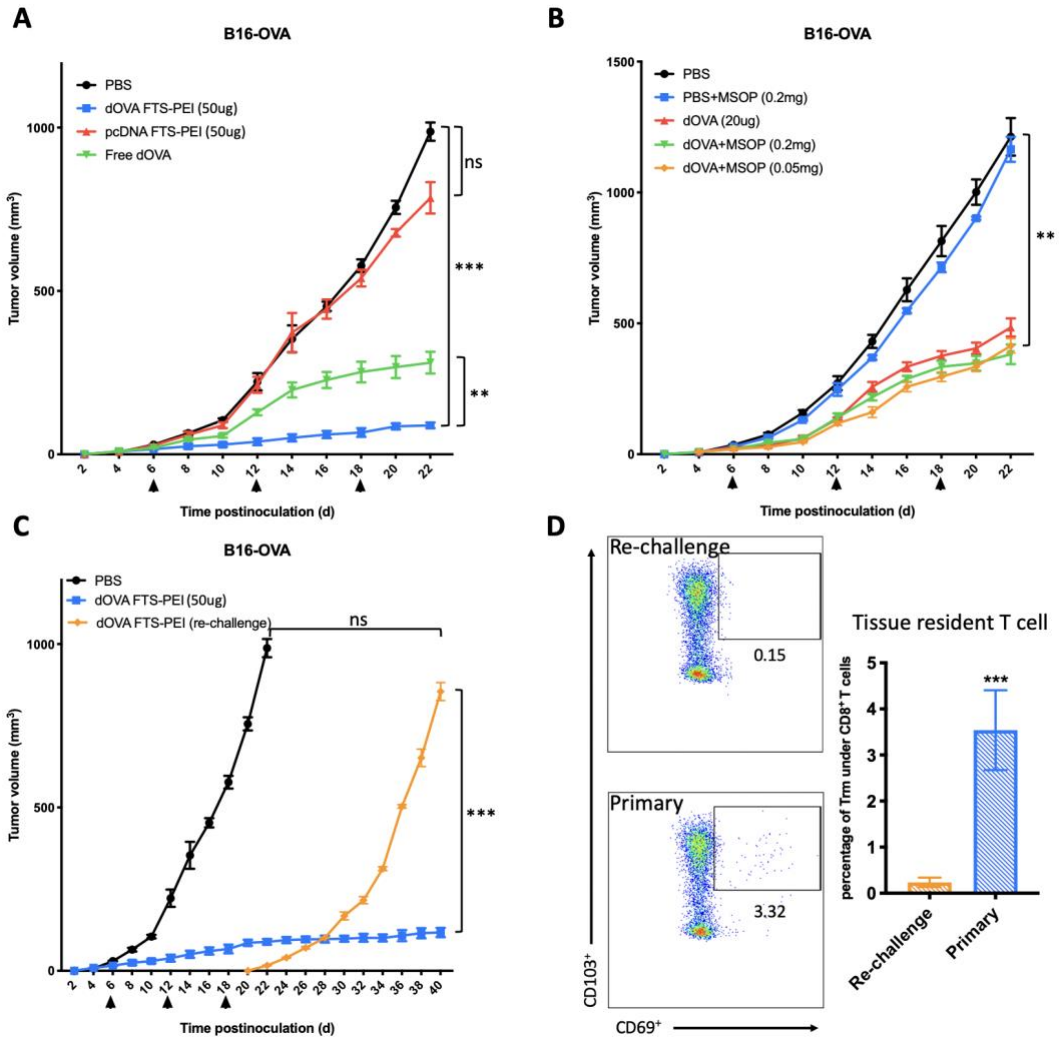

Figure. 6 PEI-FTS Nanocomplexes-Mediated Anti-tumor Immunity

(A) PBS, free OVA, PEI-FTS loaded backbone plasmid and PEI-FTS loaded OVA DNA (dOVA) were injected locally (intratumor) to B16F10-OVA bearing mice model three doses (once per 6 d). (B) MSOP co-delivery with PEI-FTS loaded dOVA to B16F10-OVA bearing mice model. (C) Re-challenge tumors were inoculated at the contralateral side 2 d after final vaccination and tumor growth in all groups were monitored 40 d after primary tumor inoculation. Values reported are the means ± SEM, n = 5. P values were generated by one-way ANOVA using the Tukey test for multiple comparisons. *P < 0.05, **P < 0.01, ***P < 0.001. (D) FACS analyses of tissue resident T cells ($CD103^+$ and $CD69^+$) in both primary and re-challenged tumors. *Gating strategy (Fig. S2):* Tissue resident T cells were first gated under Zombie NIR^- & $CD45^+$ cells indicating live tumor infiltrating lymphocytes (TILs) population and then further characeterized as the $CD8^+$ T cells highly express both tissue residency markers CD69 and CD103. Statistical analysis and data are presented as the means ± SEM, n = 5. P values were generated by two-tailed student's t-test. *P < 0.05, **P < 0.01, ***P < 0.001.

4.0 Discussion

In general, locally delivered soluble antigens or molecular adjuvants rapidly diffuse into systemic circulation such as peripheral blood vessels due to their small molecular sizes[26]. They were disseminated systemically and showed very poor targeting and accumulation in draining lymph nodes (LNs) leading to poor immune response[19]. Intratumor injection of naked nucleic acids was shown to be capable of transfecting various types of tumors but most of them were rapidly taken up by different kinds of cells through scavenger receptor-mediated endocytosis[27, 28]. As a result, only a small portion could be captured by antigen presenting cells (APCs). Its application in nonantigenic vaccination is limited by inefficient delivery to lymphoid organs to induce a potent immune response[29].

Various PEI-based nanocarriers have been developed for tumor vaccination via intratumor administration. Our PEI-FTS represents an improved transfection agent for effective gene delivery to tumors and draining lymph nodes. Vaccination via local administration can activate and stimulate “fast-response” resident T cells for local protection. Potent elicitation of antigen-specific cytotoxic T lymphocyte (CTL) responses can also be carried out by the relatively high efficiency of APC targeting mediated by the negatively charged nanocomplex[29-31].

In this study, the therapeutic application of our vaccination strategy was demonstrated using OVA as a model antigen. To facilitate its clinical translation, our next step is to further evaluate the efficacy of our strategy using wide type tumor cells instead of OVA-expressing tumor cells. Studies are currently ongoing to identify cancer cell mutations by using predictive algorithm and validation tools. Meanwhile, we are also trying to make the full use of this promising delivery

system which not only deliver nucleic acid but also co-deliver hydrophobic anti-cancer drugs through hydrophobic-hydrophobic interaction and π-π stacking to achieve combination therapy.

The underlying mechanism by which FTS enhances transfection efficiency remains unknown. Preliminary data suggested that FTS treatment can increase tumor cell transfection *in vitro* in a dose dependent manner. It is unclear whether it is attributed to changes in the biophysical properties of our carrier following modification of PEI by FTS. On the other hand, FTS is widely regarded as a RAS inhibitor, there is a possibility that RAS signaling is involved in PEI-mediated transfection[32]. Another unanswered question is why our strategy was effective in inducing a strong local antitumor activity but failed to trigger a systemic immune response to fight against distant tumors[33-36]. Finding an answer to this important question shall lead to the development of a more effective vaccination strategy for clinical application.

Appendix A Supplementary Materials

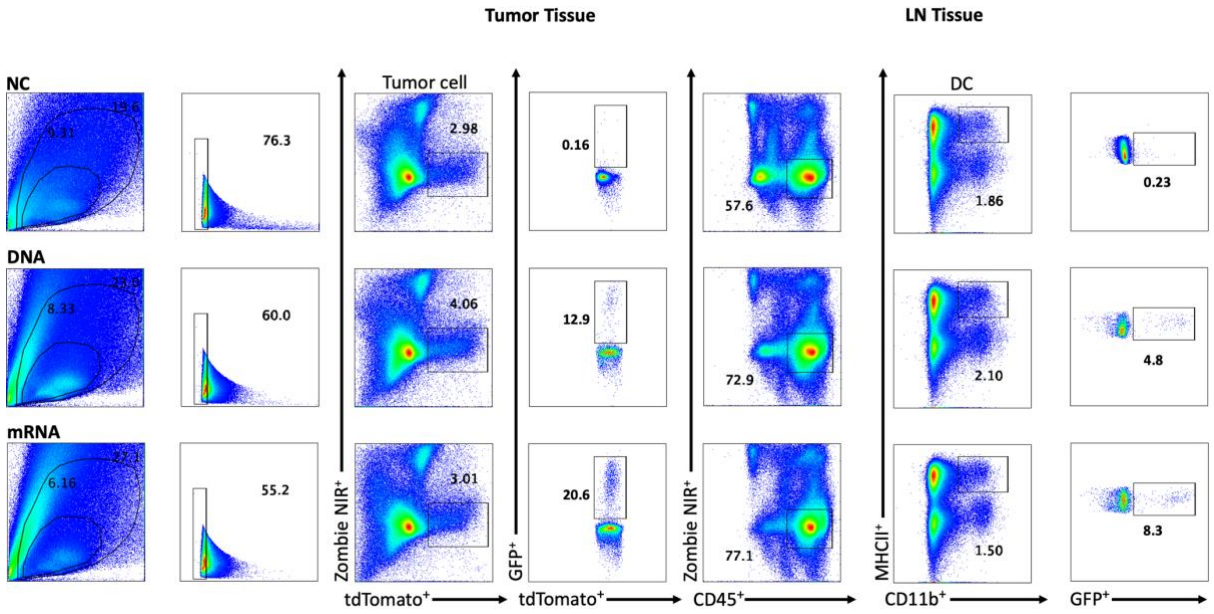

Figure. S1 Tumor Cells and Dendritic Cells Gating Strategy

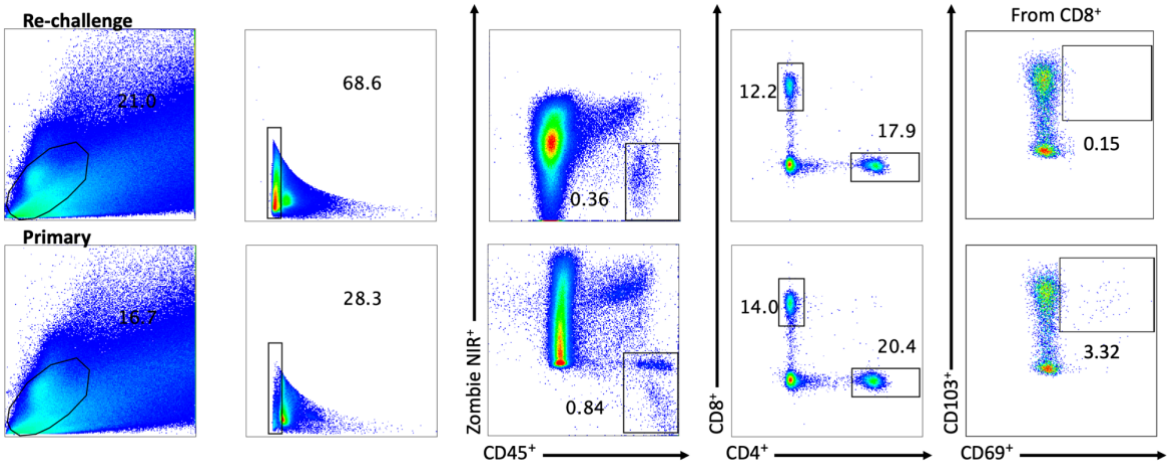

Figure. S2 Tissue Resident T Cells Gating Strategy

Bibliography

1.van der Burg, S. H.; Arens, R.; Ossendorp, F.; van Hall, T.; Melief, C. J., Vaccines for established cancer: overcoming the challenges posed by immune evasion. *Nat Rev Cancer* **2016,** *16* (4), 219-33.

2.Aldous, A. R.; Dong, J. Z., Personalized neoantigen vaccines: A new approach to cancer immunotherapy. *Bioorg Med Chem* **2018,** *26* (10), 2842-2849.

3.Melero, I.; Gaudernack, G.; Gerritsen, W.; Huber, C.; Parmiani, G.; Scholl, S.; Thatcher, N.; Wagstaff, J.; Zielinski, C.; Faulkner, I.; Mellstedt, H., Therapeutic vaccines for cancer: an overview of clinical trials. *Nat Rev Clin Oncol* **2014,** *11* (9), 509-24.

4.Efremova, M.; Finotello, F.; Rieder, D.; Trajanoski, Z., Neoantigens Generated by Individual Mutations and Their Role in Cancer Immunity and Immunotherapy. *Front Immunol* **2017,** *8*, 1679.

5.Ott, P. A.; Hu, Z.; Keskin, D. B.; Shukla, S. A.; Sun, J.; Bozym, D. J.; Zhang, W.; Luoma, A.; Giobbie-Hurder, A.; Peter, L.; Chen, C.; Olive, O.; Carter, T. A.; Li, S.; Lieb, D. J.; Eisenhaure, T.; Gjini, E.; Stevens, J.; Lane, W. J.; Javeri, I.; Nellaiappan, K.; Salazar, A. M.; Daley, H.; Seaman, M.; Buchbinder, E. I.; Yoon, C. H.; Harden, M.; Lennon, N.; Gabriel, S.; Rodig, S. J.; Barouch, D. H.; Aster, J. C.; Getz, G.; Wucherpfennig, K.; Neuberg, D.; Ritz, J.; Lander, E. S.; Fritsch, E. F.; Hacohen, N.; Wu, C. J., An immunogenic personal neoantigen vaccine for patients with melanoma. *Nature* **2017,** *547* (7662), 217-221.

6.Sahin, U.; Derhovanessian, E.; Miller, M.; Kloke, B. P.; Simon, P.; Lower, M.; Bukur, V.; Tadmor, A. D.; Luxemburger, U.; Schrors, B.; Omokoko, T.; Vormehr, M.; Albrecht, C.; Paruzynski, A.; Kuhn, A. N.; Buck, J.; Heesch, S.; Schreeb, K. H.; Muller, F.; Ortseifer, I.; Vogler, I.; Godehardt, E.; Attig, S.; Rae, R.; Breitkreuz, A.; Tolliver, C.; Suchan, M.; Martic, G.; Hohberger, A.; Sorn, P.; Diekmann, J.; Ciesla, J.; Waksmann, O.; Bruck, A. K.; Witt, M.; Zillgen, M.; Rothermel, A.; Kasemann, B.; Langer, D.; Bolte, S.; Diken, M.; Kreiter, S.; Nemecek, R.; Gebhardt, C.; Grabbe, S.; Holler, C.; Utikal, J.; Huber, C.; Loquai, C.; Tureci, O., Personalized RNA mutanome vaccines mobilize poly-specific therapeutic immunity against cancer. *Nature* **2017,** *547* (7662), 222-226.

7.Hellmann, M. D.; Snyder, A., Making It Personal: Neoantigen Vaccines in Metastatic Melanoma. *Immunity* **2017,** *47* (2), 221-223.

8.Matsushita, H.; Vesely, M. D.; Koboldt, D. C.; Rickert, C. G.; Uppaluri, R.; Magrini, V. J.; Arthur, C. D.; White, J. M.; Chen, Y. S.; Shea, L. K.; Hundal, J.; Wendl, M. C.; Demeter, R.; Wylie, T.; Allison, J. P.; Smyth, M. J.; Old, L. J.; Mardis, E. R.; Schreiber, R. D., Cancer exome analysis reveals a T-cell-dependent mechanism of cancer immunoediting. *Nature* **2012,** *482* (7385), 400-4.

9.Alexandrov, L. B.; Nik-Zainal, S.; Wedge, D. C.; Aparicio, S. A.; Behjati, S.; Biankin, A. V.; Bignell, G. R.; Bolli, N.; Borg, A.; Borresen-Dale, A. L.; Boyault, S.; Burkhardt, B.; Butler, A. P.; Caldas, C.; Davies, H. R.; Desmedt, C.; Eils, R.; Eyfjord, J. E.; Foekens, J. A.; Greaves, M.; Hosoda, F.; Hutter, B.; Ilicic, T.; Imbeaud, S.; Imielinski, M.; Jager, N.; Jones, D. T.; Jones, D.; Knappskog, S.; Kool, M.; Lakhani, S. R.; Lopez-Otin, C.; Martin, S.; Munshi, N. C.; Nakamura, H.; Northcott, P. A.; Pajic, M.; Papaemmanuil, E.; Paradiso, A.; Pearson, J. V.; Puente, X. S.; Raine, K.; Ramakrishna, M.; Richardson, A. L.; Richter, J.; Rosenstiel, P.; Schlesner, M.; Schumacher, T. N.; Span, P. N.; Teague, J. W.; Totoki, Y.; Tutt, A. N.; Valdes-

Mas, R.; van Buuren, M. M.; van 't Veer, L.; Vincent-Salomon, A.; Waddell, N.; Yates, L. R.; Australian Pancreatic Cancer Genome, I.; Consortium, I. B. C.; Consortium, I. M.-S.; PedBrain, I.; Zucman-Rossi, J.; Futreal, P. A.; McDermott, U.; Lichter, P.; Meyerson, M.; Grimmond, S. M.; Siebert, R.; Campo, E.; Shibata, T.; Pfister, S. M.; Campbell, P. J.; Stratton, M. R., Signatures of mutational processes in human cancer. *Nature* **2013,** *500* (7463), 415-21.
10.van Galen, P.; Hovestadt, V.; Wadsworth Ii, M. H.; Hughes, T. K.; Griffin, G. K.; Battaglia, S.; Verga, J. A.; Stephansky, J.; Pastika, T. J.; Lombardi Story, J.; Pinkus, G. S.; Pozdnyakova, O.; Galinsky, I.; Stone, R. M.; Graubert, T. A.; Shalek, A. K.; Aster, J. C.; Lane, A. A.; Bernstein, B. E., Single-Cell RNA-Seq Reveals AML Hierarchies Relevant to Disease Progression and Immunity. *Cell* **2019,** *176* (6), 1265-1281 e24.
11.Li, L.; Goedegebuure, S. P.; Gillanders, W. E., Preclinical and clinical development of neoantigen vaccines. *Ann Oncol* **2017,** *28* (suppl_12), xii11-xii17.
12.Kuai, R.; Ochyl, L. J.; Bahjat, K. S.; Schwendeman, A.; Moon, J. J., Designer vaccine nanodiscs for personalized cancer immunotherapy. *Nat Mater* **2017,** *16* (4), 489-496.
13.Dudek, A. M.; Martin, S.; Garg, A. D.; Agostinis, P., Immature, Semi-Mature, and Fully Mature Dendritic Cells: Toward a DC-Cancer Cells Interface That Augments Anticancer Immunity. *Front Immunol* **2013,** *4*, 438.
14.Zhang, X.; Huang, Y.; Zhao, W.; Chen, Y.; Zhang, P.; Li, J.; Venkataramanan, R.; Li, S., PEG-farnesyl thiosalicylic acid telodendrimer micelles as an improved formulation for targeted delivery of paclitaxel. *Mol Pharm* **2014,** *11* (8), 2807-14.
15.Miao, L.; Li, L.; Huang, Y.; Delcassian, D.; Chahal, J.; Han, J.; Shi, Y.; Sadtler, K.; Gao, W.; Lin, J.; Doloff, J. C.; Langer, R.; Anderson, D. G., Delivery of mRNA vaccines with heterocyclic lipids increases anti-tumor efficacy by STING-mediated immune cell activation. *Nat Biotechnol* **2019,** *37* (10), 1174-1185.
16.Zhu, G.; Zhang, F.; Ni, Q.; Niu, G.; Chen, X., Efficient Nanovaccine Delivery in Cancer Immunotherapy. *ACS Nano* **2017,** *11* (3), 2387-2392.
17.Wilson, D. S.; Hirosue, S.; Raczy, M. M.; Bonilla-Ramirez, L.; Jeanbart, L.; Wang, R.; Kwissa, M.; Franetich, J. F.; Broggi, M. A. S.; Diaceri, G.; Quaglia-Thermes, X.; Mazier, D.; Swartz, M. A.; Hubbell, J. A., Antigens reversibly conjugated to a polymeric glyco-adjuvant induce protective humoral and cellular immunity. *Nat Mater* **2019,** *18* (2), 175-185.
18.Xu, J.; Sun, J.; Ho, P. Y.; Luo, Z.; Ma, W.; Zhao, W.; Rathod, S. B.; Fernandez, C. A.; Venkataramanan, R.; Xie, W.; Yu, A. M.; Li, S., Creatine based polymer for codelivery of bioengineered MicroRNA and chemodrugs against breast cancer lung metastasis. *Biomaterials* **2019,** *210*, 25-40.
19.Liu, H.; Moynihan, K. D.; Zheng, Y.; Szeto, G. L.; Li, A. V.; Huang, B.; Van Egeren, D. S.; Park, C.; Irvine, D. J., Structure-based programming of lymph-node targeting in molecular vaccines. *Nature* **2014,** *507* (7493), 519-22.
20.Benjaminsen, R. V.; Mattebjerg, M. A.; Henriksen, J. R.; Moghimi, S. M.; Andresen, T. L., The possible "proton sponge " effect of polyethylenimine (PEI) does not include change in lysosomal pH. *Mol Ther* **2013,** *21* (1), 149-57.
21.Li, W.; Joshi, M. D.; Singhania, S.; Ramsey, K. H.; Murthy, A. K., Peptide Vaccine: Progress and Challenges. *Vaccines (Basel)* **2014,** *2* (3), 515-36.
22.Guo, Y.; Lei, K.; Tang, L., Neoantigen Vaccine Delivery for Personalized Anticancer Immunotherapy. *Front Immunol* **2018,** *9*, 1499.
23.Goldberg, M. S., Immunoengineering: how nanotechnology can enhance cancer immunotherapy. *Cell* **2015,** *161* (2), 201-4.

24.Manguso, R. T.; Pope, H. W.; Zimmer, M. D.; Brown, F. D.; Yates, K. B.; Miller, B. C.; Collins, N. B.; Bi, K.; LaFleur, M. W.; Juneja, V. R.; Weiss, S. A.; Lo, J.; Fisher, D. E.; Miao, D.; Van Allen, E.; Root, D. E.; Sharpe, A. H.; Doench, J. G.; Haining, W. N., In vivo CRISPR screening identifies Ptpn2 as a cancer immunotherapy target. *Nature* **2017,** *547* (7664), 413-418.
25.Eggermont, L. J.; Paulis, L. E.; Tel, J.; Figdor, C. G., Towards efficient cancer immunotherapy: advances in developing artificial antigen-presenting cells. *Trends Biotechnol* **2014,** *32* (9), 456-65.
26.Fifis, T.; Gamvrellis, A.; Crimeen-Irwin, B.; Pietersz, G. A.; Li, J.; Mottram, P. L.; McKenzie, I. F.; Plebanski, M., Size-dependent immunogenicity: therapeutic and protective properties of nano-vaccines against tumors. *J Immunol* **2004,** *173* (5), 3148-54.
27.Szeto, G. L.; Van Egeren, D.; Worku, H.; Sharei, A.; Alejandro, B.; Park, C.; Frew, K.; Brefo, M.; Mao, S.; Heimann, M.; Langer, R.; Jensen, K.; Irvine, D. J., Microfluidic squeezing for intracellular antigen loading in polyclonal B-cells as cellular vaccines. *Sci Rep* **2015,** *5*, 10276.
28.Ali, O. A.; Huebsch, N.; Cao, L.; Dranoff, G.; Mooney, D. J., Infection-mimicking materials to program dendritic cells in situ. *Nat Mater* **2009,** *8* (2), 151-8.
29.Alspach, E.; Lussier, D. M.; Miceli, A. P.; Kizhvatov, I.; DuPage, M.; Luoma, A. M.; Meng, W.; Lichti, C. F.; Esaulova, E.; Vomund, A. N.; Runci, D.; Ward, J. P.; Gubin, M. M.; Medrano, R. F. V.; Arthur, C. D.; White, J. M.; Sheehan, K. C. F.; Chen, A.; Wucherpfennig, K. W.; Jacks, T.; Unanue, E. R.; Artyomov, M. N.; Schreiber, R. D., MHC-II neoantigens shape tumour immunity and response to immunotherapy. *Nature* **2019,** *574* (7780), 696-701.
30.Tran, E.; Robbins, P. F.; Rosenberg, S. A., 'Final common pathway' of human cancer immunotherapy: targeting random somatic mutations. *Nat Immunol* **2017,** *18* (3), 255-262.
31.Yarchoan, M.; Johnson, B. A., 3rd; Lutz, E. R.; Laheru, D. A.; Jaffee, E. M., Targeting neoantigens to augment antitumour immunity. *Nat Rev Cancer* **2017,** *17* (4), 209-222.
32.Tran, E.; Robbins, P. F.; Lu, Y. C.; Prickett, T. D.; Gartner, J. J.; Jia, L.; Pasetto, A.; Zheng, Z.; Ray, S.; Groh, E. M.; Kriley, I. R.; Rosenberg, S. A., T-Cell Transfer Therapy Targeting Mutant KRAS in Cancer. *N Engl J Med* **2016,** *375* (23), 2255-2262.
33.Schenkel, J. M.; Masopust, D., Tissue-resident memory T cells. *Immunity* **2014,** *41* (6), 886-97.
34.Iborra, S.; Martinez-Lopez, M.; Khouili, S. C.; Enamorado, M.; Cueto, F. J.; Conde-Garrosa, R.; Del Fresno, C.; Sancho, D., Optimal Generation of Tissue-Resident but Not Circulating Memory T Cells during Viral Infection Requires Crosspriming by DNGR-1(+) Dendritic Cells. *Immunity* **2016,** *45* (4), 847-860.
35.Hailemichael, Y.; Dai, Z.; Jaffarzad, N.; Ye, Y.; Medina, M. A.; Huang, X. F.; Dorta-Estremera, S. M.; Greeley, N. R.; Nitti, G.; Peng, W.; Liu, C.; Lou, Y.; Wang, Z.; Ma, W.; Rabinovich, B.; Sowell, R. T.; Schluns, K. S.; Davis, R. E.; Hwu, P.; Overwijk, W. W., Persistent antigen at vaccination sites induces tumor-specific CD8(+) T cell sequestration, dysfunction and deletion. *Nat Med* **2013,** *19* (4), 465-72.
36.Kobold, S.; Steffen, J.; Chaloupka, M.; Grassmann, S.; Henkel, J.; Castoldi, R.; Zeng, Y.; Chmielewski, M.; Schmollinger, J. C.; Schnurr, M.; Rothenfusser, S.; Schendel, D. J.; Abken, H.; Sustmann, C.; Niederfellner, G.; Klein, C.; Bourquin, C.; Endres, S., Selective bispecific T cell recruiting antibody and antitumor activity of adoptive T cell transfer. *J Natl Cancer Inst* **2015,** *107* (1), 364.